TB64

19th International Symposium of Ballistics, 7–11 May 2001, Interlaken, Switzerland

A 3D MODELLING STUDY OF THE INFLUENCE OF SIDE WALL COLLISION ON LONG STAND-OFF JET PENETRATION

R. Cornish

Defence Evaluation and Research Agency, Fort Halstead, Sevenoaks,
Kent TN14 7BP, England UK
Tel: 44-1959-515138
email: rjcornish@dera.gov.uk

ABSTRACT

There is increasing interest in the performance of shaped charge warheads at long stand-offs in excess of 20 charge diameters. To examine the feasibility of such systems, accurate simulation of the jet penetration process at these long stand-offs is essential. Currently, analytical codes can often over estimate penetration at long stand-offs. Particle shape effects, crater clogging due to the reducing crater diameter near the end of penetration, and the effects of side wall collision as a result of off axis drift of the jet particles are candidate mechanisms that cause degradation. These mechanisms are not fully understood and are not accounted for by analytical codes. This paper focuses on the problem of side wall impact and uses a controlled modelling study, conducted in 3D, to examine some of the patterns that emerge in the long stand-off regime.

INTRODUCTION

To examine the mechanics of side wall impact, a hydrocode modelling study was undertaken using the Euler module within the DERA modelling environment, cAst. This study, which was conducted in 3D, considered a single copper particle impacting a representative side wall profile in a target of RHA under conditions appropriate to long stand-off. The copper particle, length 2 cm and width 0.4 cm, was assigned a velocity of 5 km/s. The side wall was created by cutting a hole, of diameter 3 cm, out of the RHA target. This 3D study is a follow on from a preliminary study previously conducted in plane 2D [1] to scope the task of modelling side wall impacts.

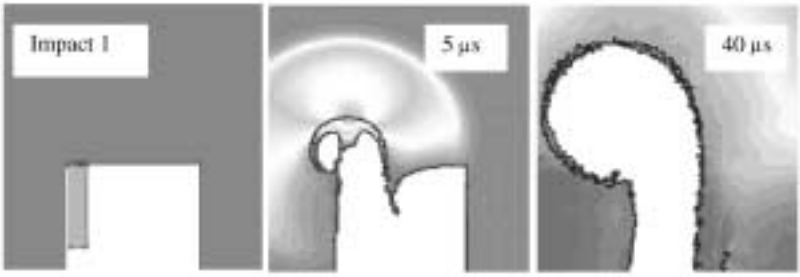

Figure 1. Plane 2D simulation, labeled Impact 1, of a square copper particle impacting the left corner of a square crater at 5 km/s.

A result of this earlier study is illustrated in Fig. 1, which shows the simulation of a rectangular copper particle, velocity 5 km/s, impacting the bottom left corner of a square crater. This simulation had a mesh resolution of 6 cells across the diameter of the jet particle, which was found to be sufficient to accurately resolve the impact. For ease of presentation in the following sections, this result is labeled Impact 1. The initial set up of the simulation is shown on the left of the figure and the penetration sequence is shown toward the right at an intermediate time of 5 μs and a final time of 40 μs, where penetration has finished. A strong shock wave is observed at 5 us during penetration. The crater attains its final shape at the end of the penetration process when the stresses have fallen below the yield stress of the RHA. It should be noted that the images in Fig. 1 have been clipped to fit on the page. In each case the target was made wide enough to ensure that boundary conditions did not influence the penetration.

Since this simulation was undertaken in plane 2D, Fig. 1 effectively represents an infinite rectangular cord impacting into the corner of an infinite rectangular groove. This means that the stresses will be more severe than for a true jet particle impact, since the shock wave induced in the target has only a 2D space to decay into. In reality, jet particle penetration is a 3D problem and this shock wave will decay in 3D. While the 2D study was not wholly representative of a true side wall impact, it was considered to give a good indication of the trends in the mechanisms of side wall impact. The results of the 2D study indicated the potential for side wall impacts to be significant in influencing the progress of subsequent particle impacts. This finding was considered important enough to warrant a full 3D analysis to study the mechanics of side wall impact in greater detail. This work focused firstly on identifying the influence of particle shape and crater shape on the outcome of long stand-off penetration. Following this, work was undertaken to identify some of the side wall impact mechanisms that could lead to the production of clutter, i.e. material that will interfere with following parts of the jet. In both cases, the emphasis was on identifying trends and simple rules that may eventually be used within analytical codes to give improved prediction of long stand-off jet penetration.

EFFECT OF PARTICLE SHAPE AND CRATER SHAPE ON PENETRATION

One of the key reasons why shape effects are important relates to the way semi-empirical codes calculate jet penetration. It is common for such codes to simplify both the jet and the target crater so that the penetration may be calculated. It is usual for these codes to represent a jet particle as being either cylindrical or elliptical in shape. The separate contributions to the final crater, caused by individual jet particles are normally represented as cylindrical craters whose axes are aligned with the axis of penetration of the contributing particle. The depths of these cylinders are calculated using the classical hydrodynamic penetration law for compressible flow. It was decided that some 3D simulations should be undertaken to identify the influence of particle shape and crater shape in jet particle penetration.

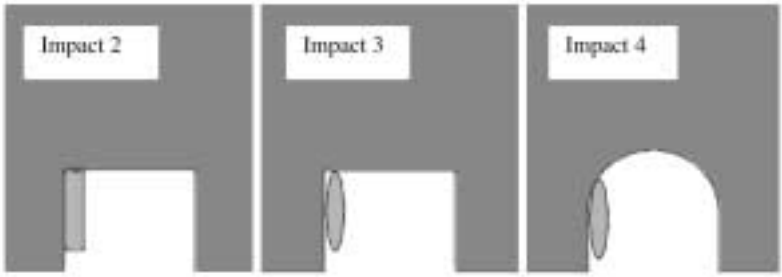

Figure 2. Initial set up of the 3D simulations, Impact 2, Impact 3 and Impact 4, which investigate the influence of particle shape and crater shape on penetration.

The 3D study considered a copper particle, 0.4 cm diameter, 2 cm long, impacting the side wall of a representative crater, 3 cm in diameter, within an RHA target. Three cases were studied, as shown in Fig. 2. The first, Impact 2, considered a cylindrical particle impacting the bottom of a flat cylindrical crater. The second, Impact 3, considered an elliptical particle impacting the bottom of a flat cylindrical crater. The third, Impact 4, examined an elliptical particle impacting the bottom of a rounded cylindrical crater. In the latter case the bottom of the crater was considered to be spherical. The depths of the craters were set so that the volume of each crater was the same. The purpose of fixing the volume was that this is the most likely approach an analytical code would use to relate a square crater profile to a rounded one. In each case the particle was made to have the same length and diameter as the cylindrical particle. The reason for preserving these parameters instead of the overall particle mass is that it is these parameters that are most easily measurable on an X-ray radiograph of a jet.

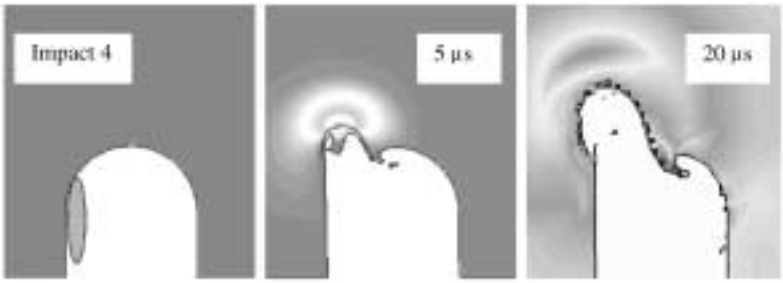

Figure 3. 3D simulation, Impact 4, of an elliptical particle impacting the left hand side of a rounder crater at 5 km/s.

The penetration sequence for the elliptical particle impacting the rounded crater is shown in Fig. 3. This time the shock generated by the impact decays much more rapidly since it is decaying in 3D. This means that, overall, the stresses are much lower that in the 2D simulation, Fig. 1, and the crater produced is much narrower. Consequently, it is only necessary to run the simulation to 20 μs. The final crater profiles obtained from each simulation are compared below in Fig 4a and b, where the crater from the 2D simulation, Impact 1, has been added for reference. Note that the results are compared in two ways. Fig. 4a compares the crater profiles where the results have been aligned to the initial crater profiles, at time zero. This gives a comparison of the relative final crater depths that are produced. By contrast, Fig. 4b compares the results where the cater profiles have been off set so that, at time zero, the tips of each particle are aligned. This compares the amount of target material each particle has actually penetrated.

Fig. 4a, shows that the crater obtained from the 2D simulation, Impact 1, has, for the reasons explained above produced a much wider crater than its 3D equivalent, Impact 2. The net depths of penetration for these two impacts, however, are almost the same. This is expected since the analyitic formulae that estimate penetration depth are identical for both the 2D and 3D cases, despite their differing geometries. It is seen that Impact 3, identical to Impact 2, but with an elliptical particle, has a slightly narrower crater and a lower penetration depth. This is unsurprising as the elliptical particle has less mass than its cylindrical counterpart. Impact 4, identical to Impact 3, but with a rounded crater has a slightly lower penetration depth still. This time the lower penetration depth occurs because the particle is off set due to the rounded geometry, of the crater, initially being further away from the bottom of the crater, Fig. 2. Consequently, impact 4 is always at a disadvantage in terms of absolute penetration depth. This difference in initial particle position needs to be accounted in any analysis of relative performance.

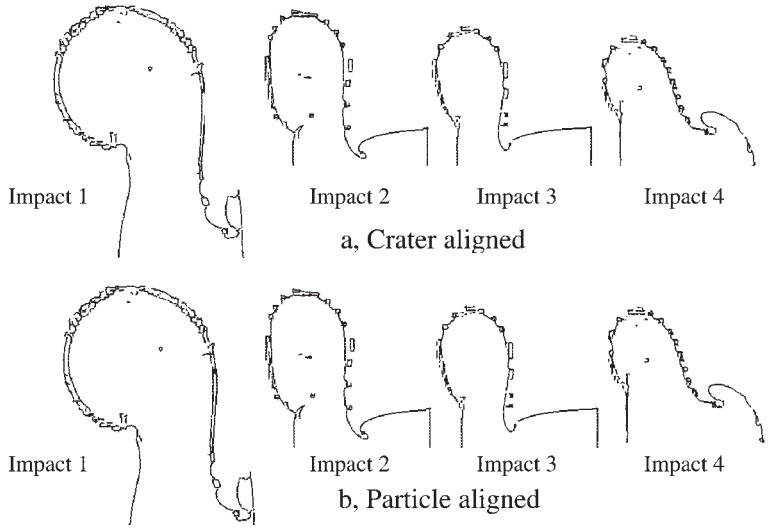

Figure 4. Comparison for Impact 1 to Impact 4 of the final crater profiles where, (a) the profiles are aligned according to the initial crater positions, and (b) the profiles are aligned according to the initial particle positions.

Examining Fig. 4b, which shows the amount of target material each particle penetrates, it is seen that the profiles of Impacts 3 and 4 are now of identical height. This means that for both the flat crater and the rounded crater, the particle has actually penetrated the same amount of material.

THE EFFECT OF IMPACT LOCATION ON SIDE WALL PENETRATION

A major concern in jet penetration at long stand-off is the potential for interaction between jet particles and side-wall material to produce clutter which can inhibit further penetration. As yet, semi-empirical codes do not account for such behavior in their penetration calculations. To address this issue, some 3D simulations were undertake to examine side wall impacts at four separate locations to identify instances of clutter and their influence on penetration. The first two locations considered impacts at the bottom of the crater, as depicted in Fig. 5, Impacts 5 and 6. The first of these occurs at the side of the crater and the second occurs at one third of a crater diameter. The next two locations, Fig. 5, Impacts 7 and 8, considered side wall impact occurring at these same radial positions but at an intermediate position along the depth of the crater, as opposed to the bottom of the crater. The alignment of the particle in Impact 8 was devised so that the particle would impact on the corner edge of the crater profile. To provide a reference for comparison, a further simulation, Impact 9, which considered the case of ideal, on-axis penetration, at the bottom of the crater was run. This reference simulation was conducted as a 2D axi-symmetric calculation.

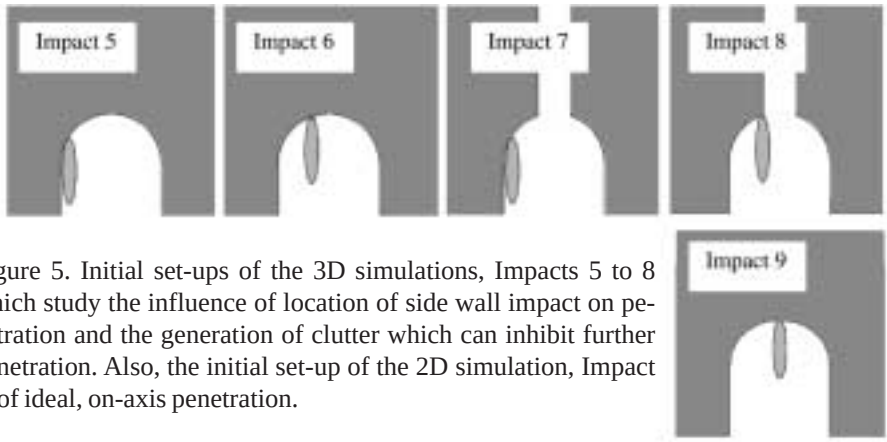

Figure 5. Initial set-ups of the 3D simulations, Impacts 5 to 8 which study the influence of location of side wall impact on penetration and the generation of clutter which can inhibit further penetration. Also, the initial set-up of the 2D simulation, Impact 9, of ideal, on-axis penetration.

The results of Impacts 5 and 6, at the bottom of the crater, are compared with the result for ideal penetration, Impact 9, in Fig. 6a and b. As before, the profiles have been aligned to separately compare the overall penetration depth, Fig. 6a and the amount of target material penetrated by the impacting particle, Fig. 6b. Fig. 6a, shows that both off-axis profiles are of similar width and volume to the ideal penetration profile. The off-axis profiles appear slightly angled away from the vertical, due to the extra material to their left that was available to provide additional confinement. This is most noticeable for Impact 5, which occurred at the side of the crater. This impact also produced the least overall penetration, with both off-axis profiles showing less overall penetration than the ideal, on-axis penetration. This reduction in penetration with off-axis position is due almost entirely to the fact that the off-axis particles had to begin penetrating from positions that were geometrically offset from the bottom of the crater. This is shown, in Fig. 6b, where it is seen that despite the varying radial location of the impact, the amount of target material actually penetrated by each particle is the same. A similar trend has been observed for a lower impact velocity of 2 km/s. Again the differences in net penetration depth are due mainly to the differences in initial off-set of the particles. At such low velocities, however, material strength begins to play more of a role in the penetration This means that the amount of target material penetrated by each material is no longer exactly the same and the on-axis particle now penetrates slightly higher than its off-axis counterparts. While this is so, the difference is small, and is within 5%.

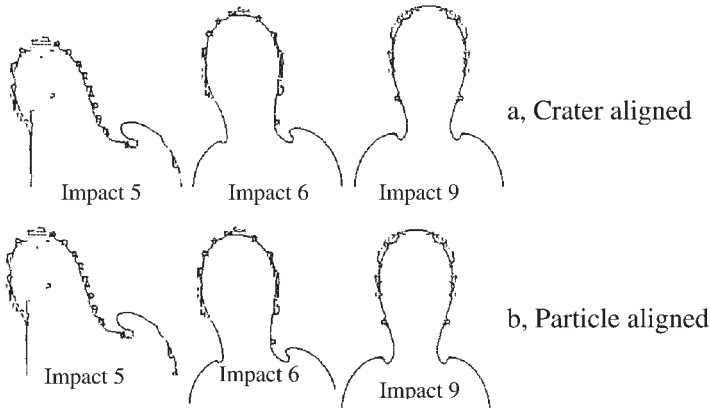

Figure 6. Comparison for Impact 5, 6 and 9 of the final crater profiles where, (a) the profiles are aligned according to the initial crator positions, and (b) the profiles are aligned accordning to the initial particle positions.

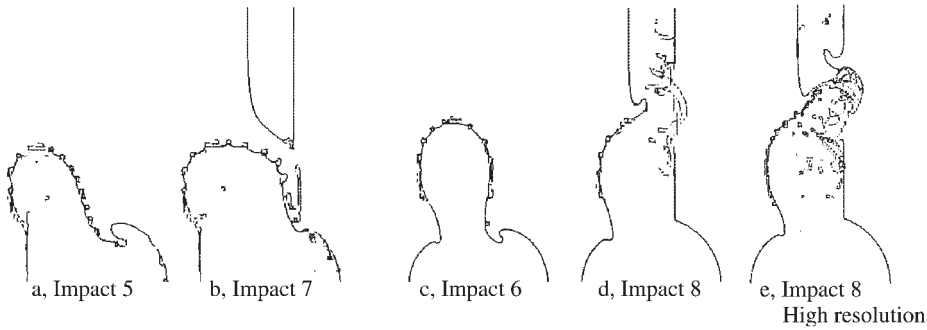

Figure 7. Comparison of final crater profiles for impact at the side of the crater occurring, (a), at the bottom of the crater, Impact 5, and, (b) part way down the crater, Impact 7, and impact at one third of the crater's diameter, occurring, (c), at the bottom of the crater Impact 6, and (d), part way down the crater, Impact 8. The profile, (e) for, impact 8 at a higher resolution of 8 cells across the particle is also shown.

It is next useful to examine how each of the off-axis penetrations described above would have appeared if they occurred part way down the crater instead of at the bottom. This is illustrated in Fig. 7a to e. Figs. 7a and b compare penetrations at the side wall occurring at the bottom of the crater, a, and part way down the crater, b. It is seen that overall penetration depths are the same. Thus the reduction in confinement to the right for Impact 7 due to the initial crater on the right hand side of penetration has had an insignificant effect on the depth of penetration. The dramatic feature that Fig 7b shows is that this confining material has splayed outward and blocked the crater. It is likely that this material will seriously inhibit the influence of a subsequent particle.

Fig. 7c and d compare penetrations at one third of a crater diameter, occurring at the bottom of the crater, c, and part way down the crater, d. For the latter case, an extra profile is presented, e, where a higher mesh resolution, of 10 cells across the particle diameter, as

opposed to 6, was used. The similarity between the profiles of Fig. 7d and e demonstrates that 6 cells resolution is sufficient for the purposes of this study. Looking at the overall penetration along the axis of impact, it is seen that the penetration depth is the same for both impact locations. Slightly to right of this axis, the penetration is a bit deeper for impact 8, due to the lesser confinement available on this side. The interesting feature of this result, identified by a more thorough analysis, is that in this impact, the particle, which has impacted the corner edge of the crater, actually produces a small jet which shoots off to the right and impacts the wall on the opposite side of the crater. The aftermath is seen as a small tunnel that has been bored out of this opposite side in the crater wall. This is particularly noticeable at the higher mesh resolution. Figs. 7d and e show that this interaction has caused a small amount of ejecta to be present in the crater. This dynamic material could potentially inhibit the effect of a successive particle, but probably only to a very minor degree.

CONCLUSIONS

The influence of particle shape and crater shape on penetration have been identified where the shapes considered were chosen to reflect the way analytical codes model penetration. Some simple patterns have emerged which can be used to assist the development of improved algorithms for modelling long stand-off penetration.

Some examples of off-axis penetration that lead to the production of clutter have been identified. In one case, the impact into the side wall led to a large amount of target material being forced inwards towards the center of the crater. This material is likely to severely impede the penetration of a subsequent particle.

REFERENCES

1 R. Cornish, J. T. Mills, J. P. Curtis and D. Finch. “Degradation Mechanisms in Shaped Charge Jet Penetration”. Proceedings of the Hypervelocity Impact Symposium, Galverton, Texas, USA, Nov 2000. To be published in Int. J. Impact Eng, Vol. 26, 2001